

OPTIMIZATION OF ESPRIT ALGORITHM AND FAST DOA ESTIMATION FOR UNIFORM LINEAR ARRAYS

XinYu Weng

Tianjin University of Technology and Education, Tianjin 300222, China.

Abstract: To tackle the problems of high computational complexity and cumbersome engineering deployment posed by traditional subspace-based direction-of-arrival (DOA) estimation algorithms, this study presents a low-complexity DOA estimation approach designed specifically for uniform linear arrays (ULA). The key innovation of the proposed method is the elimination of eigenvalue decomposition or singular value decomposition (EVD/SVD)—two core components of classical subspace-based techniques. Instead, it employs a strategy of array segmentation and matrix reconstruction. In detail, the ULA is first split into two separate subarrays, and their cross-covariance matrix is used to build a joint cross-covariance matrix. An equivalent signal subspace is then directly generated via a linear transformation, which greatly simplifies the computational procedure. Finally, by exploiting the rotation invariance principle of ESPRIT, the proposed approach realizes fast and precise DOA estimation. Theoretical analyses and simulation results indicate that, in comparison with traditional subspace-based algorithms, the proposed method reduces computational complexity significantly while retaining comparable estimation accuracy, thus improving the overall efficiency of DOA estimation.

Keywords: DOA estimation; Joint cross-covariance matrix; Signal subspace; ESPRIT algorithm

1 INTRODUCTION

Direction-of-arrival (DOA) estimation is a fundamental task in array signal processing, with broad applications in radar systems, wireless communications, and geophysical exploration [1-5]. Accurate and real-time DOA estimation is critical for enhancing target detection performance, positioning precision, and overall system robustness. With the continuous advancement of array signal processing technologies, there is an increasing demand for low-complexity and high-precision algorithms that can operate reliably in complicated electromagnetic environments and support large-scale antenna configurations. The field has evolved considerably from early parameter estimation schemes to modern super-resolution approaches, among which subspace-based methods have greatly improved both estimation accuracy and angular resolution. Representative methods in this category include the Multiple Signal Classification (MUSIC) algorithm and the Estimation of Signal Parameters via Rotational Invariance Techniques (ESPRIT) algorithm [6, 7]. Conventional subspace-based schemes typically rely on eigenvalue decomposition (EVD) or singular value decomposition (SVD) of the sample covariance matrix to separate signal and noise subspaces [8]. Furthermore, the MUSIC algorithm involves an exhaustive spectral peak search, which introduces excessive computational complexity and creates significant challenges for real-time engineering applications.

To alleviate the computational burden of subspace-based DOA estimation methods, a variety of reliable alternative approaches have been developed in existing research. The ROOT-MUSIC algorithm substitutes spectral peak search with polynomial rooting, which reduces computational complexity for small-scale arrays [9-12]. Nevertheless, its computational requirements remain high due to its ongoing reliance on EVD and the rising order of the polynomial as the number of array elements increases. A distinct method proposed by Yeh Chien-Chung constructs a low-dimensional projection matrix using any K rows of the covariance matrix (where K denotes the number of signal sources), allowing angle estimation through a reduced-dimensional search function [13]. The Propagator Method (PM) avoids eigendecomposition entirely by constructing the noise subspace via linear operations, though it suffers from significant performance degradation under low signal-to-noise ratio (SNR) conditions [14].

For large-scale arrays, a single-snapshot algorithm accomplishes DOA estimation by dividing the array into multiple subarrays, requiring only one data snapshot [15]. Another technique reconstructs the covariance matrix with specific structural constraints—low-rank, Toeplitz, and positive semidefinite—and then employs Vandermonde decomposition for DOA estimation [16]. While this method avoids complex EVD/SVD computations and enhances processing speed, its use is restricted to uniform and sparse rectangular arrays. For L-shaped arrays, the CESA algorithm extracts specific elements from the covariance matrix to build an equivalent signal subspace, enabling two-dimensional (2D) DOA estimation without eigendecomposition [17]. Yan et al. extended this concept to uniform linear arrays (ULA) with the JCCM algorithm, which obtains direction-of-arrival (DOA) information by processing the first column of the joint cross-covariance matrix [18]. Nevertheless, the construction of the signal subspace in this approach still leaves room for further optimization.

In conclusion, existing subspace-based DOA estimation methods are still largely limited by traditional matrix computation frameworks. They struggle to balance computational efficiency and estimation accuracy without relying on eigen decomposition—a key bottleneck that hinders their practical engineering applications. To overcome these critical limitations, this paper proposes a fast DOA estimation algorithm that integrates the core principles of ESPRIT, CESA,

and JCCM [7, 17, 18]. The proposed method is theoretically based on array segmentation and matrix reconstruction techniques. First, the ULA is split into two independent subarrays, and their received data are used to calculate a reliable joint cross-covariance matrix. By applying a series of reasonable transformations to the first column of this matrix, an equivalent signal subspace is effectively established, completely eliminating the need for EVD or SVD that are essential to traditional subspace-based methods and significantly reducing computational complexity. Subsequently, DOA estimation is achieved quickly and accurately by utilizing the rotational invariance property of the ESPRIT algorithm. Simulation results show that the proposed algorithm offers significant advantages in computational complexity while maintaining estimation performance comparable to that of traditional methods in practical scenarios.

2 SIGNAL MODEL

The As illustrated in Figure 1, we consider the following array receiving model: suppose there exist K mutually independent far-field narrowband signal sources with carrier wavelength λ , which impinge on a uniform linear array (ULA) composed of $2N$ isotropic and uniformly spaced elements. The incident angles of these sources are denoted as $\theta_k(k=1,2,\dots,K)$, satisfying the condition $2N>K$. We partition the ULA into two subarrays, each containing N elements, referred to as Subarray 1 and Subarray 2 respectively, with the leftmost element serving as the phase reference point. Based on this configuration, the received signal vectors of the two subarrays at time t can be expressed as:

$$\mathbf{x}_1(t) = \mathbf{A}(\theta)\mathbf{s}(t) + \mathbf{n}_1(t) \tag{1}$$

$$\mathbf{x}_2(t) = \mathbf{A}(\theta)\mathbf{\Phi}\mathbf{s}(t) + \mathbf{n}_2(t) \tag{2}$$

where $\mathbf{x}_1(t)=[\mathbf{x}_1(t), \mathbf{x}_2(t), \dots, \mathbf{x}_N(t)]^T$ and $\mathbf{x}_2(t)=[\mathbf{x}_{N+1}(t), \mathbf{x}_{N+2}(t), \dots, \mathbf{x}_{2N}(t)]^T$ represent the received signal vectors of Subarray 1 and Subarray 2, respectively.

$\mathbf{s}(t)$ is the signal vector, which can be expressed as:

$$\mathbf{s}(t)=[s_1(t), s_2(t), \dots, s_k(t)]^T \tag{3}$$

$\mathbf{n}_1(t)$ and $\mathbf{n}_2(t)$ represent the additive Gaussian white noise vectors of Subarray 1 and Subarray 2, respectively, expressed as:

$$\mathbf{n}_1(t)=[n_1(t), n_2(t), \dots, n_N(t)]^T \tag{4}$$

$$\mathbf{n}_2(t)=[n_{N+1}(t), n_{N+2}(t), \dots, n_{2N}(t)]^T \tag{5}$$

The subarray steering matrix can be expressed as

$$\mathbf{A}(\theta)=[\mathbf{a}(\theta_1), \mathbf{a}(\theta_2), \dots, \mathbf{a}(\theta_k)] \tag{6}$$

where $\mathbf{a}(\theta_k)=[1, e^{-j2\pi d \sin \theta_k / \lambda}, \dots, e^{-j2\pi d (N-1) \sin \theta_k / \lambda}]$;

$\mathbf{\Phi}$ is a $K \times K$ diagonal matrix, whose diagonal elements are the phase delays of the K signals between any pair of array elements, expressed as

$$\mathbf{\Phi} = \begin{pmatrix} e^{jN\mu_1} & & & \\ & \ddots & & \\ & & & e^{jN\mu_k} \end{pmatrix} \tag{7}$$

where $\mu_k = 2\pi d \sin \theta_k / \lambda, k = 1, 2, \dots, K$.

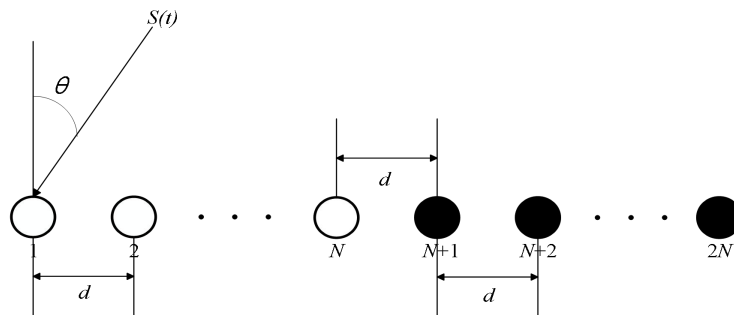


Figure 1 Receiving Data Model

3 FAST DOA ESTIMATION BASED ON UNIFORM ARRAYS

3.1 Proposed Algorithm

Let the cross-covariance matrix between the received signals of Subarray 1 and Subarray 2 be denoted as \mathbf{R}_{12} , and the cross-covariance matrix between the received signals of Subarray 2 and Subarray 1 be denoted as \mathbf{R}_{21} . From equations (1) and (2), the following relationship can be derived:

$$\begin{aligned}\mathbf{R}_{12} &= E\{\mathbf{x}_1(t)\mathbf{x}_2^H(t)\} = \mathbf{A}(\theta)E\{\mathbf{s}(t)\mathbf{s}^H(t)\}\mathbf{\Phi}^H\mathbf{A}^H(\theta) + E\{\mathbf{n}_1(t)\mathbf{n}_2^H(t)\} \\ &= \mathbf{A}(\theta)\mathbf{R}_s\mathbf{\Phi}^H\mathbf{A}^H(\theta)\end{aligned}\quad (8)$$

$$\begin{aligned}\mathbf{R}_{21} &= E\{\mathbf{x}_2(t)\mathbf{x}_1^H(t)\} = \mathbf{A}(\theta)E\{\mathbf{s}(t)\mathbf{s}^H(t)\}\mathbf{\Phi}^H\mathbf{A}^H(\theta) + E\{\mathbf{n}_2(t)\mathbf{n}_1^H(t)\} \\ &= \mathbf{A}(\theta)\mathbf{R}_s\mathbf{\Phi}^H\mathbf{A}^H(\theta)\end{aligned}\quad (9)$$

In the formula: $\mathbf{R}_s = E\{\mathbf{s}(t)\mathbf{s}^H(t)\}$. Since the defined signals are independent and uncorrelated, the auto-covariance matrix \mathbf{R}_s of the signals is a diagonal matrix, with diagonal elements corresponding one-to-one to the signal energy, i.e.

$$\mathbf{R}_s = \text{diag}(p_1, p_2, \dots, p_K) \quad (10)$$

Where $p_i (i=1,2,\dots,K)$ represents the energy of the i -th signal. Similarly, noises $\mathbf{n}_1(t)$ and $\mathbf{n}_2(t)$ are statistically independent, $E\{\mathbf{n}_1(t)\mathbf{n}_2^H(t)\} = 0$, so the interference of additive noise is effectively suppressed. At this point, the combined cross-covariance matrix can be expressed as:

$$\mathbf{R} = \mathbf{R}_{12} + \mathbf{R}_{21} = \mathbf{A}(\theta)\mathbf{R}_s(\mathbf{\Phi}^H + \mathbf{\Phi})\mathbf{A}^H(\theta) \quad (11)$$

Where $\mathbf{R}_s(\mathbf{\Phi}^H + \mathbf{\Phi})$ can be written as:

$$\mathbf{R}_s(\mathbf{\Phi}^H + \mathbf{\Phi}) = \begin{bmatrix} \xi_1 & 0 & \dots & 0 \\ 0 & \xi_1 & \dots & \vdots \\ \vdots & \vdots & \vdots & 0 \\ 0 & \dots & 0 & \xi_K \end{bmatrix} = \mathbf{\Lambda} \quad (12)$$

Among them, $\xi_i \stackrel{\Delta}{=} p_i(e^{-j\mu_i} + e^{j\mu_i}), i=1,2,\dots,K$. Since the signal energy p_i is a positive real number, ξ_i is also a positive real number, and it can be deduced that $\mathbf{\Lambda} = \mathbf{\Lambda}^*$. As the elements in the first column of $\mathbf{A}^H(\theta)$ are all 1, define a K -dimensional all-1 column vector \mathbf{L} . Represent the first column elements of \mathbf{R} with an M -dimensional column vector $\mathbf{r}(:,1)$, that is, $\mathbf{r}(:,1) = \mathbf{A}(\theta)\mathbf{\Lambda}\mathbf{L}$; based on $\mathbf{r}(:,1)$, define a new column vector $\mathbf{r}^n(:,1) = \mathbf{D}\mathbf{r}^*((:,1))$, where

$$\mathbf{D} = \begin{bmatrix} & & & 1 \\ & \cdot & \cdot & \\ & & & \\ 1 & & & \end{bmatrix} \quad (13)$$

Use $\mathbf{r}(:,1)$ and $\mathbf{r}^n(:,1)$ to construct a $2N$ -dimensional column vector:

$$\mathbf{r} = \begin{bmatrix} \mathbf{r}^n(:,1) \\ \mathbf{r}(:,1) \end{bmatrix} = \begin{bmatrix} \mathbf{D}\mathbf{A}^*(\theta) \\ \mathbf{A}(\theta) \end{bmatrix} \mathbf{\Lambda}\mathbf{L} \quad (14)$$

Since the elements in the first row of $\mathbf{A}(\theta)$ and the elements in the last row of $\mathbf{D}\mathbf{A}^*(\theta)$ are the same, deleting one of the rows yields a $(2N-1)$ -dimensional column vector:

$$\mathbf{r}_{new} = \begin{bmatrix} e^{j2\pi(N-1)d\sin\theta_1/\lambda} & \dots & e^{j2\pi(N-1)d\sin\theta_k/\lambda} \\ \vdots & \dots & \vdots \\ 1 & \dots & 1 \\ \vdots & \dots & \vdots \\ e^{-j2\pi(N-1)d\sin\theta_1/\lambda} & \dots & e^{-j2\pi(N-1)d\sin\theta_k/\lambda} \end{bmatrix} \begin{bmatrix} \alpha_1 \\ \alpha_2 \\ \vdots \\ \alpha_k \end{bmatrix} = \bar{\mathbf{A}}(\theta)\mathbf{a} \quad (15)$$

Obviously, \mathbf{r}_{new} corresponds to the data obtained from a single sampling of $2N-1$ array elements. Based on \mathbf{r}_{new} , a $(2N-K) \times K$ matrix \mathbf{S} is constructed, expressed as:

$$\mathbf{S} = [r_1, r_2, \dots, r_k] \quad (16)$$

Where $\mathbf{r}_i = \mathbf{r}_{new}(i:2N-K-1+i), i=1,2,\dots,k$, and $\mathbf{r}_{new}(u:v)$ denotes the column vector composed of the u -th to v -th rows of \mathbf{r}_{new} . From Equations (15) and (16), we obtain:

$$\mathbf{S} = \mathbf{G}\mathbf{A}\mathbf{Q} \quad (17)$$

where

$$\mathbf{G} = \begin{bmatrix} e^{j2\pi(N-1)d\sin\theta_1/\lambda} & \dots & e^{j2\pi(N-1)d\sin\theta_k/\lambda} \\ \vdots & \dots & \vdots \\ 1 & \dots & 1 \\ \vdots & \dots & \vdots \\ e^{-j2\pi(N-K)d\sin\theta_1/\lambda} & \dots & e^{-j2\pi(N-K)d\sin\theta_k/\lambda} \end{bmatrix} \quad (18)$$

It is clear that both \mathbf{G} and \mathbf{Q} are Vandermonde matrices. Given that the incident signals are mutually uncorrelated, matrices \mathbf{G} and \mathbf{A} are column full-rank, while \mathbf{Q} is row full-rank—each having a rank equal to the number of signal sources K . Consequently, the column space of \mathbf{G} is identical to that of \mathbf{S} , i.e., $\text{span}(\mathbf{G})=\text{span}(\mathbf{S})$. Notably, \mathbf{S} embeds the DOA information of the incident signals. Furthermore, applying the Schmidt orthogonalization procedure to the column vectors of \mathbf{S} yields the full signal subspace $\bar{\mathbf{S}}$.

$$\bar{\mathbf{S}} = \mathbf{A}\mathbf{T} \tag{19}$$

and $\bar{\mathbf{S}}$ can also be divided into upper and lower parts.

$$\bar{\mathbf{S}} = \begin{bmatrix} \mathbf{U}_1 \\ \mathbf{U}_2 \end{bmatrix} = \begin{bmatrix} \mathbf{A}\mathbf{T} \\ \mathbf{A}\Phi\mathbf{T} \end{bmatrix} \tag{20}$$

From the preceding equation, we obtain: $\mathbf{U}_2 = \mathbf{U}_1 \mathbf{T}^{-1} \Phi \mathbf{T} = \mathbf{U}_1 \Psi \mathbf{T}$. This leads to the conclusion that the column spaces spanned by \mathbf{U}_1 and \mathbf{U}_2 are equivalent, i.e., $\text{span}(\mathbf{U}_1)=\text{span}(\mathbf{U}_2)$. Moreover, Φ and Ψ re similar matrices, with the diagonal entries of Φ a corresponding to the eigenvalues of Ψ . This indicates that we only need to solve for Ψ , and then perform eigenvalue decomposition on Ψ to retrieve the DOA estimates[19,20].

3.2 Computational Complexity Analysis

his section analyzes the computational complexity of the proposed algorithm and benchmarks it against the methods presented in ESPRIT [7], Fast root MUSIC [9], and JCCM [13]. Letting the number of snapshots be T , the total number of array elements be $2N$, and the number of signal sources be K , we adopt the number of complex multiplications as the primary metric for evaluating computational complexity. The computational complexity of the algorithm in ESPRIT [7] is primarily dominated by $O[4N^2 T+4K^2 (2N-I)+8N^3+2K^3+K^3]$; the complexity of the algorithm in Fast root MUSIC [9] is mainly $O[4N^2 T+8N^3+(K+I)^2]$; the complexity of the algorithm in JCCM [13] is mainly $O[4NT+2(K^2 +K)(2N-K)^2/2 +8(2N-K-I)^3]$. The computational complexity of the proposed algorithm in this paper is mainly concentrated in the acquisition of $\mathbf{r}(:,1)$, Schmidt orthogonalization, and one eigenvalue decomposition. Thus, the computational complexity of the proposed algorithm is $O[4NT+ 2(K^2+K)(2N-K)^2/2+K^3]$.

4 EXPERIMENTAL VERIFICATION AND COMPARISON

In this section, we conduct comparative simulation experiments to evaluate the performance differences between the proposed method and several existing algorithms, including ESPRIT [7], Fast root MUSIC, and JCCM [13]. We adopt the root mean square error (RMSE) of estimation outputs as the primary metric to assess each algorithm’s estimation accuracy, where V represents the total number of Monte Carlo trials and K denotes the number of incident signal sources. The RMSE is defined as follows:

$$RMSE = \sqrt{\frac{1}{KV} \sum_{v=1}^V \sum_{k=1}^K (\tilde{\eta}_k^{(v)} - \eta_k)^2}, \eta = \theta \tag{21}$$

4.1 DOA Estimation Simulation Experiment

Figure 2 verifies the signal processing capability of the algorithm proposed in this paper. Assume that two uncorrelated far-field narrowband signals impinge on a uniform linear array with a total of 16 array elements (i.e., 8 elements in both Subarray 1 and Subarray 2). The true angle parameters are set as $\theta=[-30^\circ, -15^\circ, 5^\circ, 22^\circ]$. The number of snapshots is set to 2000, and the signal-to-noise ratio (SNR) is set to 20 dB. Figure 2 shows that the proposed algorithm can successfully identify the four signals.

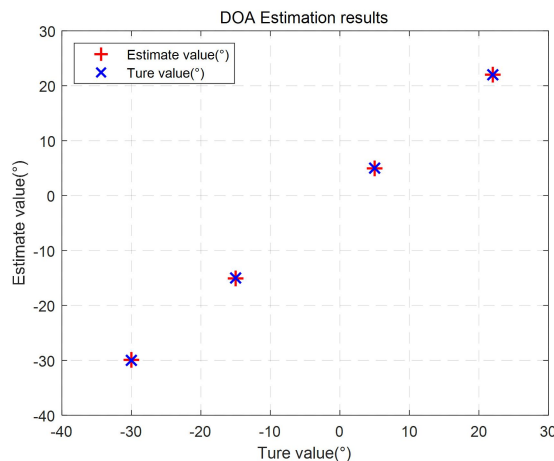


Figure 2 DOA Estimation Result

Figure 3 illustrates how the root mean square error (RMSE) performance of various methods varies with Signal-to-Noise Ratio (SNR). In this simulation, two uncorrelated far-field narrowband signals impinge on a uniform linear array (ULA) consisting of 16 elements (with 8 elements in each of Subarray 1 and Subarray 2), and their incident angles are set to $\theta = [-15^\circ, 22^\circ]$. The snapshot count is fixed at 400, and the SNR is swept from 0 dB to 20 dB in increments of 2 dB. We perform 1000 independent Monte Carlo trials to compute the RMSE for each method. Figure 3 presents the comparison of DOA estimation accuracy across algorithms under different SNR levels. The results demonstrate that, relative to the algorithms in ESPRIT [7], Fast root MUSIC [9], and JCCM [13], the proposed method achieves comparable parameter estimation precision while incurring lower computational complexity.

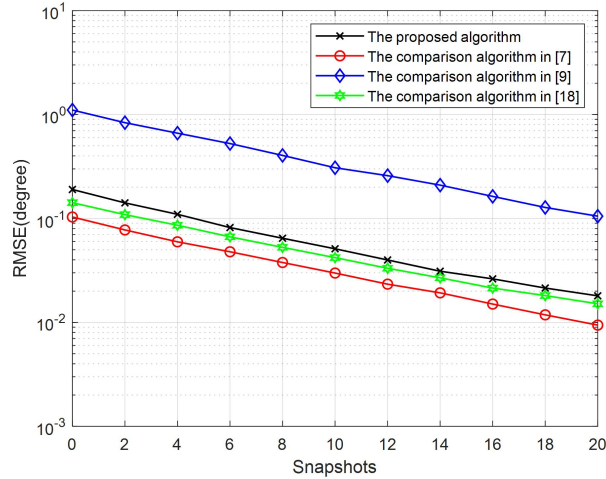


Figure 3 SNR VS RMSE Simulation Results

Figure 4 illustrates how the root mean square error (RMSE) performance of various methods changes with the number of sampling snapshots. In this simulation setup, two uncorrelated far-field narrowband signals impinge on a uniform linear array (ULA) containing 16 elements (with 8 elements in each of Subarray 1 and Subarray 2), and their incident angles are configured as $\theta = [-15^\circ, 22^\circ]$. The Signal-to-Noise Ratio (SNR) is fixed at 5 dB, and the snapshot count is swept from 100 to 1000 in increments of 100. We conduct 1000 independent Monte Carlo trials to compute the RMSE for each algorithm. Figure 4 presents the comparison of DOA estimation accuracy across methods under different snapshot numbers. The results indicate that, relative to the algorithms presented in ESPRIT [7], Fast root MUSIC [9], and JCCM [13], the proposed method delivers comparable parameter estimation precision while boasting lower computational complexity.

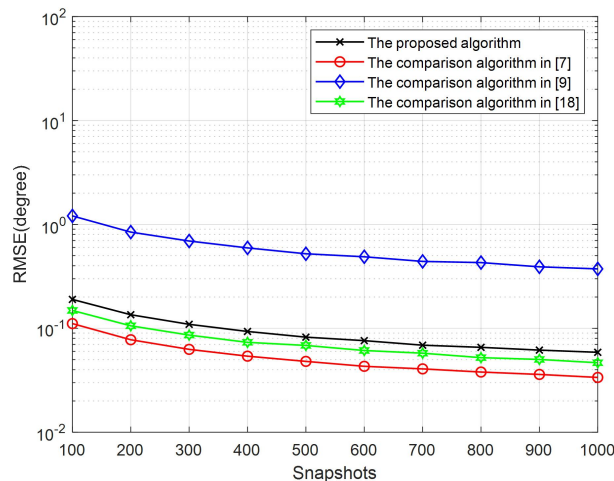


Figure 4 Number of Snapshots vs RMSE Simulation Results

4.2 DOA Estimation Simulation Experiment

Figure 5 validates the computational complexity of the proposed algorithm against those of ESPRIT [7], Fast root MUSIC [9], and JCCM [13] for varying numbers of array elements N . In this evaluation, the number of array elements N ranges from 0 to 50 with an increment of 5, while the number of signal sources is fixed at $K=3$. The number of snapshots is set to 100, and the number of complex multiplications is used as the primary metric for complexity evaluation. Figure 5 plots the computational complexity curves of the proposed method and the benchmark algorithms, i.e., ESPRIT [7], Fast root MUSIC [9], and JCCM [13]. The results show that as the array scale increases, the computational complexity of the proposed algorithm remains lower than that of the comparative methods. This result

further corroborates the validity of the theoretical performance analysis presented in Section 2.

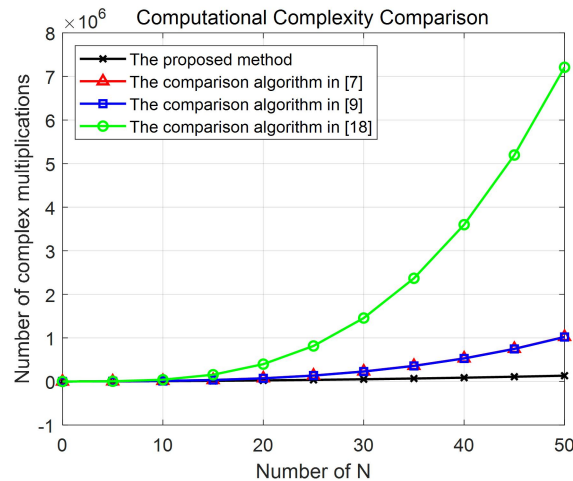


Figure 5 Comparison of Computational Complexity under Different Numbers of Array Elements N

5 CONCLUSION

This work presents an efficient direction-of-arrival estimation algorithm tailored for uniform linear arrays, with two core innovations that address critical limitations of conventional subspace-based methods. First, an equivalent signal subspace is constructed by processing the first column entries of the cross-covariance matrix, eliminating the computationally burdensome eigenvalue decomposition or singular value decomposition operations inherent in classical approaches, which significantly reduces the computational overhead and avoids numerical instability issues often encountered in large-scale array scenarios. Second, by leveraging the rotational invariance property of array manifolds, the algorithm avoids the need for exhaustive spectral peak searches or polynomial rooting operations, enabling rapid and accurate DOA estimation with minimal computational cost. Simulation results demonstrate that the proposed algorithm achieves a notable reduction in computational complexity while preserving satisfactory angle estimation precision, even under low signal-to-noise ratio (SNR) conditions, rendering it well-suited for real-time large-scale antenna array application scenarios such as 5G communications and radar systems. Nevertheless, practical engineering implementations frequently require the retrieval of two-dimensional (2D) signal angle parameters; thus, extending the proposed algorithm to 2D scenarios with L-shaped or rectangular arrays remains an area that demands further in-depth investigation and development to fully meet the demands of modern wireless communication and radar systems.

COMPETING INTERESTS

The authors have no relevant financial or non-financial interests to disclose.

REFERENCES

- [1] Liu Wei, Haardt Martin, Greco Maria S, et al. Twenty-Five Years of Sensor Array and Multichannel Signal Processing: A review of progress to date and potential research directions. *IEEE Signal Processing Magazine*, 2023, 40(4): 80-91.
- [2] Chen Hua, Lin Hongguang, Liu Wei, et al. Augmented Multi-Subarray Dilated Nested Array With Enhanced Degrees of Freedom and Reduced Mutual Coupling. *IEEE Transactions on Signal Processing*, 2024, 72: 1387-1399.
- [3] Xu Zhengguang, Chen Yaling, Zhang Peng. A Sparse Uniform Linear Array DOA Estimation Algorithm for FMCW Radar. *IEEE Signal Processing Letters*, 2023, 30: 823-827.
- [4] Li Ping, Li Jianfeng, Zhao Gaofeng. Low complexity DOA estimation for massive UCA with single snapshot. *Journal of Systems Engineering and Electronics*, 2022, 33(1): 22-27.
- [5] Tian Quan, Cai Ruiyan. A Low-Complexity DOA Estimation Algorithm for Distributed Source Localization. *IEEE Transactions on Instrumentation and Measurement*, 2023, 72: 1-4.
- [6] Schmidt R. Multiple emitter location and signal parameter estimation. *IEEE Transactions on Antennas and Propagation*, 1986, 34(3): 276-280.
- [7] Yang Zai. Nonasymptotic Performance Analysis of ESPRIT and Spatial-Smoothing ESPRIT. *IEEE Transactions on Information Theory*, 2023, 69(1): 666-681.
- [8] Hussain Ahmed A, Tayem Nizar, Soliman Abdel-Hamid. Low Complexity DOA Estimation of Multiple Coherent Sources Using a Single Direct Data Snapshot. *IEEE Access*, 2024, 12: 2371-2388.
- [9] Ren QS, Willis AJ. Fast root MUSIC algorithm. *Electronics letters*, 1997, 33(6): 450-451.
- [10] Veerendra D, Niranjana K R, Malik Iram, et al. Modified Root-MUSIC Algorithm for Target Localization Using Nyström Approximation. *IEEE Sensors Journal*, 2024, 24(8): 13209-13216.

- [11] Qian Yang, Han Xiaolei, Shi Xinlei, et al. Direct position determination of non-Gaussian sources for sensor arrays via improved rooting subspace data fusion method. *IEEE Sensors Journal*, 2023, 23(20): 25307-25315.
- [12] Liu Aihua, Zhang Xin, Yang Qiang, et al. Combined root-MUSIC algorithms for multi-carrier MIMO radar with sparse uniform linear arrays. *IET Radar, Sonar & Navigation*, 2019, 13(1): 89-97.
- [13] Yeh Chien-Chung. Simple computation of projection matrix for bearing estimations. *IEE Proceedings F (Communications, Radar and Signal Processing)*, 1987, 134(2): 146-150.
- [14] Marcos S, Marsal A, Benidir M. Performances analysis of the propagator method for source bearing estimation. *Proceedings of ICASSP '94. IEEE International Conference on Acoustics, Speech and Signal Processing*, 1994, 4: 237-240.
- [15] Bressner T A H, Johannsen U, Smolders A B. Single shot DoA estimation for large-array base station systems in multi-user environments. *Loughborough Antennas & Propagation Conference (LAPC 2017)*, Loughborough, UK, 2017: 1-4.
- [16] Tian Xiyan, Lei Jinhui, Du Liufeng. A Generalized 2-D DOA Estimation Method Based on Low-Rank Matrix Reconstruction. *IEEE Access*, 2018, 6: 17407-17414.
- [17] Xi Nie, Li Liping. A Computationally Efficient Subspace Algorithm for 2-D DOA Estimation with L-shaped Array. *IEEE Signal Processing Letters*, 2014, 21(8): 971-974. DOI: 10.1109/LSP.2014.2321791
- [18] Yan Fenggang, Rong Jiajia, Liu Shuai, et al. Joint cross-covariance matrix based fast direction of arrival estimation. *Systems Engineering and Electronics*, 2018, 40(4): 733-738.
- [19] Lawal Teslim, Ofuzim Onyero Walter. Total Least Squares Implementation of ESPRIT Algorithm for Signal Processing. 2024.
- [20] Chen Chen, Zhang Zhengyi, Lian Haisheng. A Low-Complexity Joint Angle Estimation Algorithm for Weather Radar Echo Signals Based on Modified ESPRIT. *Journal of Industrial Engineering and Applied Science*, 2025, 3(2): 33-43.